

# Cationic, Two-Coordinate Gold $\pi$ Complexes

Rachel E. M. Brooner and Ross A. Widenhoefer\*

alkene ligands · allenes · gold · ligand effects ·  
structure elucidation

**C**ationic, two-coordinate gold  $\pi$  complexes that contain a phosphine or *N*-heterocyclic supporting ligand have attracted considerable attention recently owing to the potential relevance of these species as intermediates in the gold-catalyzed functionalization of C–C multiple bonds. Although neutral two-coordinate gold  $\pi$  complexes have been known for over 40 years, examples of the cationic two-coordinate gold(I)  $\pi$  complexes germane to catalysis remained undocumented prior to 2006. This situation has changed dramatically in recent years and well-defined examples of two-coordinate, cationic gold  $\pi$  complexes containing alkene, alkyne, diene, allene, and enol ether ligands have been documented. This Minireview highlights this recent work with a focus on the structure, bonding, and ligand exchange behavior of these complexes.

## 1. Introduction

The proliferation of gold(I)-catalyzed methods for the functionalization of C–C multiple bonds represents one of the most significant developments in homogeneous catalysis over the past decade.<sup>[1–3]</sup> During this period, focus has transitioned steadily from Lewis-acidic gold(III) catalysts to ligand-stabilized cationic gold(I) catalysts owing to their desirable combination of high  $\pi$  acidity and low oxophilicity. While many synthetically useful transformations have emerged from these efforts, cationic gold(I) complexes have demonstrated particular utility as catalysts for the functionalization of C–C multiple bonds.<sup>[1–3]</sup> Notable among these are the cycloaddition of enynes and related substrates,<sup>[2]</sup> and the hydrofunctionalization of C–C multiple bonds with carbon and heteroatom nucleophiles.<sup>[3]</sup> Mechanisms involving outer-sphere addition of a nucleophile to a cationic, two-coordinate gold(I)  $\pi$  complex are typically invoked for these transformations (Scheme 1),<sup>[1–3]</sup> although direct experimental evidence is limited.<sup>[4–6]</sup>

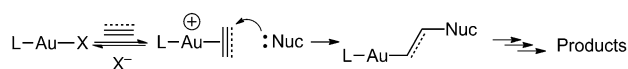
Neutral, two-coordinate gold  $\pi$  complexes have been known for over 40 years,<sup>[7]</sup> and three-coordinate gold  $\pi$  complexes for almost 20 years.<sup>[8]</sup> In contrast, well-characterized examples of the cationic two-coordinate gold(I)  $\pi$  complexes germane to catalysis remained unknown until recently.<sup>[9]</sup> In

the absence of experimental data, information regarding the structure and bonding of cationic, two-coordinate gold  $\pi$  complexes was derived primarily from several computational studies involving the hypothetical gold ethylene and acetylene complexes  $\text{Au}(\text{C}_2\text{H}_4)^+$  and  $\text{Au}(\text{C}_2\text{H}_2)^+$ , respectively.<sup>[10]</sup>

These analyses point to a significant electrostatic component of the gold–substrate bond with the covalent component dominated by  $\sigma$  donation from the filled ethylene  $\pi$  orbital to an empty gold atomic orbital. Contribution of  $\pi$  backbonding to the gold–ligand interaction is presumably attenuated by the large energy difference between the gold 5d and alkene  $\pi^*$  orbitals and by the positive charge on gold. More recent computational analyses largely support this picture of the gold– $\pi$  ligand interaction.<sup>[11]</sup> As a notable exception, Tarantelli and co-workers argued on the basis of an electron-charge displacement analysis that  $\pi$  backbonding is an important component of the gold– $\pi$  ligand bond.<sup>[12]</sup>

In 2006 Echavarren and co-workers reported the isolation and structural characterization of a family of cationic, two-coordinate gold  $\pi$ -arene complexes,<sup>[13]</sup> and shortly thereafter Sadighi and co-workers reported isolation of a cationic, two-coordinate gold  $\pi$ -alkyne complex.<sup>[14]</sup> These reports represent the leading edge of what has become an active area of research directed toward the experimental investigation of cationic, two-coordinate gold  $\pi$  complexes, which now includes  $\pi$ -alkene,  $\pi$ -alkyne,  $\pi$ -diene,  $\pi$ -allene, and  $\pi$ -arene complexes. As compared to neutral two-coordinate gold  $\pi$  complexes, cationic, two-coordinate gold  $\pi$  complexes are

[\*] R. E. M. Brooner, Prof. R. A. Widenhoefer  
French Family Science Center, Duke University  
Durham, NC 27708-0346 (USA)  
E-mail: rwidenho@chem.duke.edu



**Scheme 1.** General mechanism for gold(I)  $\pi$ -activation catalysis involving a cationic, two-coordinate gold  $\pi$  complex.

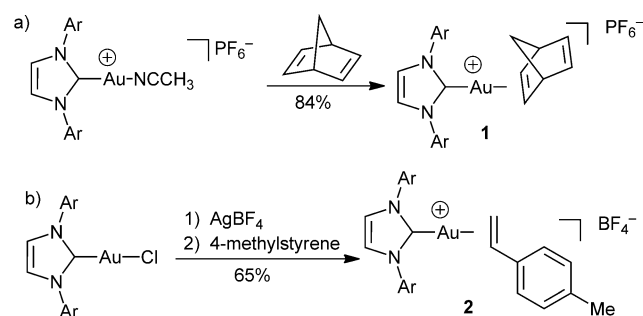
more electrophilic and more thermally stable. In comparison, three-coordinate gold  $\pi$  complexes, both neutral and cationic, are significantly more stable and more electron rich than are cationic two-coordinate gold  $\pi$  complexes.<sup>[9]</sup>

Herein, we highlight the experimental studies of cationic two-coordinate gold  $\pi$  complexes with a focus on structure, spectroscopy, particularly as it relates to electronic structure, and inter- and intramolecular  $\pi$ -ligand exchange. The review is organized globally according to  $\pi$ -ligand type and further organized according to the supporting ligand when relevant. Within each subheading the material is typically presented chronologically. Unless noted otherwise, each  $\pi$ -ligand section deals only with aliphatic and aromatic  $\pi$  ligands. Heteroatom-substituted  $\pi$  ligands are treated separately owing to their markedly different binding properties. Not included are  $\sigma$ ,  $\pi$ - and *gem*-diaurated complexes,<sup>[15]</sup> and computational results are noted only if particularly relevant.

## 2. $\pi$ -Alkene Complexes

### 2.1. N-Heterocyclic Carbene Complexes

In 2009, Nolan and co-workers reported isolation of the gold norbornadiene (NBD) complex  $[(\text{IPrAu}(\eta^2\text{-NBD}))][\text{PF}_6^-]$  (**1**) from the reaction of  $[(\text{IPrAu}(\text{NCCH}_3))][\text{PF}_6^-]$  with norbornadiene (Scheme 2a). The complex **1** was characterized in solution but decomposed by P–F bond cleavage to form  $[(\text{IPrAu})_2(\mu\text{-PF}_4)][\text{PF}_4^-]$  upon attempted crystallization.<sup>[16]</sup> Similarly, Macchioni and co-workers reported isolation of the gold styrene complex  $[(\text{IPrAu}(\eta^2\text{-4-methylstyrene}))][\text{BF}_4^-]$  (**2**) from reaction of 4-methyl styrene



**Scheme 2.** Synthesis of the IPr gold  $\pi$ -alkene complexes **1** and **2** (Ar = 2,6-diisopropylphenyl).

with a mixture of  $(\text{IPr})\text{AuCl}$  and  $\text{AgBF}_4$  (Scheme 2b).<sup>[17]</sup> Low-temperature  $^{19}\text{F}$ ,  $^1\text{H}$  HOESY NMR of **2** and related gold N-heterocyclic carbene (NHC) complexes indicated that the  $\text{BF}_4^-$  counterion is positioned predominantly (65–83 % occupancy) near the IPr imidazole ring remote from the  $\pi$  ligand.<sup>[17,18]</sup> Brown, Dickens, and Widenhoefer subsequently reported the synthesis of a diverse family of air- and thermally-stable complexes of the form  $[(\text{IPr})\text{Au}(\pi\text{ alkene})][\text{SbF}_6^-]$  [alkene = isobutylene (**3a**), 2,3-dimethyl-2-butene (**3b**), norbornene, 2-methyl-2-butene, methylenecyclohexane, *cis*-2-butene, 1-hexene, and 4-methylstyrene; Figure 1].<sup>[19]</sup> This study included solution and solid-state characterization, analysis of alkene binding affinities, and ligand exchange kinetics.

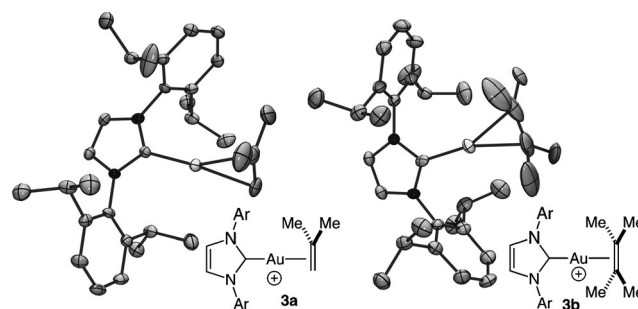


**Figure 1.** Skeletal representations and ORTEP diagrams of complexes **3a** and **3b**. Hydrogen atoms and counterions are omitted for clarity (Ar = 2,6-diisopropylphenyl). Thermal ellipsoids shown at 50 % probability.

In the  $^{13}\text{C}$  NMR spectra of IPr gold  $\pi$ -alkene complexes, the resonances for the  $\text{sp}^2$ -carbon atoms of symmetric internal alkenes and the terminal  $\text{sp}^2$ -carbon atoms of 1-alkenes were shielded relative to the free alkene. In the case of 1,1-disubstituted alkene complexes such as **3a**, the resonance of the terminal  $\text{sp}^2$ -carbon atom was shifted strongly upfield ( $\Delta\delta = -20$ ) while that of the internal  $\text{sp}^2$ -carbon atom was shifted downfield ( $\Delta\delta = 12$ ), thus pointing to slippage of gold toward the unsubstituted alkene terminus. Importantly, the  $^1J_{\text{C}=\text{C}}$  coupling constant of the isobutylene ligand of **3a** was diminished by only 5 Hz relative to free isobutylene, thus pointing to minimal deviation of the bound isobutylene from  $\text{sp}^2$  hybridization and hence nominal contribution of  $\pi$  back-bonding to the gold–alkene bond.<sup>[19]</sup> In the solid state, IPr



Ross A. Widenhoefer received his B.A. in chemistry from Gustavus Adolphus College (St. Peter, Minnesota, USA) in 1989. He received his Ph. D. degree from the University of Wisconsin-Madison in 1994 under the direction of Prof. C. P. Casey and was an NCI postdoctoral trainee at MIT in the laboratories of Prof. S. L. Buchwald. In 1997 he joined the faculty at Duke University and currently holds the rank of Professor of Chemistry.



Rachel Brooner received her B.A. in Chemistry from Huntingdon College (Montgomery, Alabama, USA) in 2008. She is currently a fifth-year graduate student in the laboratory of Prof. Ross Widenhoefer at Duke University studying the mechanisms of  $\pi$  activation catalyzed by gold(I) complexes and Brønsted acids.

gold  $\pi$ -alkene complexes adopt distorted linear geometries [C(carbene)-Au-C=C(centroid): 172–177°] with no significant elongation of the coordinated C=C bond relative to the free alkene (Figure 1).<sup>[19]</sup> Consistent with the <sup>13</sup>C NMR spectroscopy, the gold  $\pi$ -isobutylene complex **3a** displayed significant slippage of gold toward the less-substituted alkene terminus, thus binding through a shorter Au–CH<sub>2</sub> and a longer Au–CMe<sub>2</sub> bond ( $\Delta d = 0.086$  Å). In comparison, the Au–C bonds of complex **3b** differed by less than 0.01 Å.

Kinetic analysis of intermolecular isobutylene exchange with **3a** established an [isobutylene]-dependent pathway with an energy barrier of  $\Delta G^\ddagger_{318\text{K}} = 16$  kcal mol<sup>−1</sup> arising from a modest enthalpy of activation ( $\Delta H^\ddagger = 8$  kcal mol<sup>−1</sup>) and large negative entropy of activation ( $\Delta S^\ddagger = -27$  eu). These data are consistent with an associative pathway for isobutylene exchange involving the cationic bis(alkene) intermediate [(IPr)Au( $\eta^2$ -H<sub>2</sub>C=CMe<sub>2</sub>)<sub>2</sub>][SbF<sub>6</sub>]. Toward further evaluating the  $\sigma$ -donation/ $\pi$ -backbonding nature of the gold–alkene bond, Widenhoefer, Dickens, and Brown determined the relative binding affinities of *p*-substituted vinyl arenes to the 12-electron gold fragment [(IPr)Au]<sup>+</sup>.<sup>[19]</sup> A plot of log *K*<sub>eq</sub> versus the Hammett  $\sigma$  parameter produced a reaction constant of  $\rho = -2.4 \pm 0.2$ , which is significantly more negative than those obtained for the binding of vinyl arenes to cationic Ag<sup>I</sup> ( $\rho = -0.77$ ),<sup>[20]</sup> Pt<sup>II</sup> ( $\rho = -1.32$ ),<sup>[21]</sup> and Pd<sup>II</sup> ( $\rho \approx -1.4$ ) fragments.<sup>[22]</sup> These observations indicated that the bonding interaction for cationic gold alkene complexes is biased toward  $\sigma$  donation and away from  $\pi$  backbonding to an extent unprecedented for late-transition-metal  $\pi$ -alkene complexes.

## 2.2. Hindered Alkyl Phosphine Complexes

### 2.2.1. Monophosphine Complexes

Concurrent with Widenhoefer's report of IPr gold  $\pi$ -alkene complexes, Green, Russell, and co-workers reported the synthesis of gold complexes of the form [(PtBu<sub>3</sub>)Au( $\pi$  alkene)][SbF<sub>6</sub>] [alkene = isobutylene (**4a**), norbornene, norbornadiene, *trans*-cyclooctene; Figure 2].<sup>[23]</sup> Subsequently, Brown, Dickens, and Widenhoefer reported the isolation of eleven compounds of the form [(P1)Au( $\pi$  alkene)][SbF<sub>6</sub>] [P1 = P(*t*Bu)<sub>2</sub>*o*-biphenyl; Figure 2].<sup>[24]</sup> As compared to the IPr gold complex **3a**, solid-state analysis of the 1,1-disubstituted alkene complexes **4a** and [(P1)Au( $\pi$  methylenecyclohexane)][SbF<sub>6</sub>] (**5a**) revealed more pronounced slippage of the alkene ligand toward the unsubstituted terminus [ $\Delta d$  Au–CH<sub>2</sub>/Au–CR<sub>2</sub> = 0.126 (**4a**) and 0.155 Å (**5a**); Figure 2]. Also

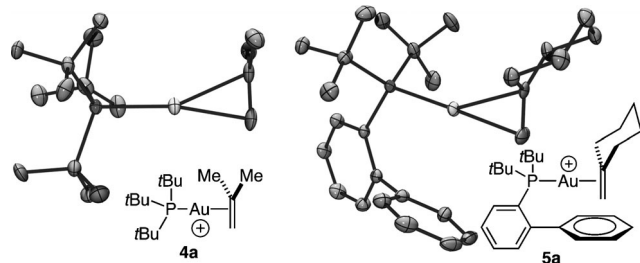


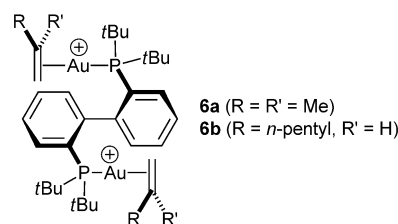
**Figure 2.** Skeletal representations and ORTEP diagrams of **4a** and **5a**. Hydrogen atoms and counterion omitted for clarity. Thermal ellipsoids shown at 50% probability.

evident from X-ray structural analysis was the pronounced steric influence of the protruding phenyl ring of the P1 ligand, which was manifested in the more significant deviation from linearity [P–Au–C=C(centroid): 161–165°] relative to both the PtBu<sub>3</sub> and IPr complexes. The more pronounced slippage of the 1,1-disubstituted alkene ligand of the gold phosphine complexes **4a** and **5a** relative to the IPr complex **3a** was also reflected by the more significant downfield shift of the internal resonances of the sp<sup>2</sup>-carbon atoms of **4a** and **5a** ( $\Delta\delta = 20$  ppm) relative to free alkene in the <sup>13</sup>C NMR spectra.

Kinetic analysis of intermolecular isobutylene exchange with [(P1)Au( $\pi$ -H<sub>2</sub>C=CMe<sub>2</sub>)]<sup>+</sup>[SbF<sub>6</sub>]<sup>−</sup> (**5b**) established the presence of an [isobutylene]-dependent pathway with activation parameters ( $\Delta H^\ddagger = 5$  kcal mol<sup>−1</sup>,  $\Delta S^\ddagger = -33$  eu) similar to those of the IPr complex **3a**.<sup>[19]</sup> Hammett analysis of the binding affinities of substituted vinyl arenes to the 12-electron gold fragment [(P1)Au]<sup>+</sup> produced a reaction constant of  $\rho = -3.4$ , which significantly exceeded that determined for the binding of vinyl arenes to [(IPr)Au]<sup>+</sup>. This observation and those outlined in the preceding paragraph point to the greater electrophilicity of the [(L)Au]<sup>+</sup> (L = P1, PtBu<sub>3</sub>) gold fragment relative to [(IPr)Au]<sup>+</sup>.

### 2.2.2. Bis(phosphine) Complexes

As an entry point into understanding the catalytic behavior of bis(gold) complexes containing an axially chiral bis(phosphine) ligand, Widenhoefer and Brooner reported the synthesis and solid-state structures of the dicationic, bis(gold)  $\pi$ -alkene complexes [(P-P)Au( $\eta^2$ -alkene)<sub>2</sub>][2SbF<sub>6</sub>] [alkene = isobutylene (**6a**), 1-pentene (**6b**); Scheme 3].<sup>[25]</sup> Although the 1-pentene complex **6b** crystallized as a single diastereomer, **6b** existed in solution as a statistical 1:2:1 mixture of diastereomers, thus indicating no influence of the chiral ligand framework on the  $\pi$ -face selectivity of binding. However, *K*<sub>eq</sub> for displacement of the first NCAR<sub>F</sub> [NCAR<sub>F</sub> = 4-NCC<sub>6</sub>H<sub>4</sub>(CF<sub>3</sub>)] ligand from [(P-P)Au(NCAR<sub>F</sub>)<sub>2</sub>][2SbF<sub>6</sub>] with isobutylene was five-times greater than the *K*<sub>eq</sub> for displacement of the second, thus indicating that isobutylene complexation is affected by the environment of the proximal gold center.

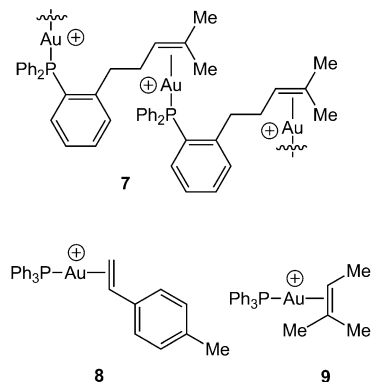


**Scheme 3.** Dicationic, bis(gold)  $\pi$ -alkene complexes containing a bis(phosphine) ligand.

## 2.3. Triarylphosphine Complexes

In contrast to gold complexes containing NHC and hindered alkylphosphine ligands, well-defined examples of

cationic gold  $\pi$ -alkene complexes containing triarylphosphine ligands have proven elusive. In 2008, Shapiro and Toste reported the synthesis of the polymeric, cationic gold  $\pi$ -alkene complex **7** which contained a triarylphosphine ligand tethered to a trisubstituted alkene moiety (Scheme 4).<sup>[26]</sup> Single-crystal X-ray analysis of **7** established the presence of a distorted gold  $\pi$ -alkene bond with a shorter Au–CHR and a longer Au–CMe<sub>2</sub> interaction ( $\Delta d = -0.1$  Å), but there was no evidence that the gold alkene bond of **7** persisted in solution.



**Scheme 4.** Cationic gold  $\pi$ -alkene complexes containing triarylphosphine supporting ligands.

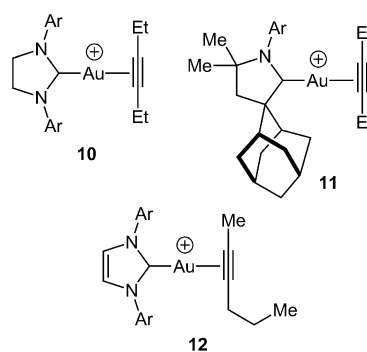
In 2009, Macchioni and co-workers reported in situ generation of the triphenylphosphine gold 4-methylstyrene complex  $[\text{Ph}_3\text{PAu}(\eta^2\text{-H}_2\text{C=CH-4-C}_6\text{H}_4\text{CH}_3)][\text{BF}_4]$  (**8**·BF<sub>4</sub>), which was characterized without isolation at or below  $-20^\circ\text{C}$  (Scheme 4).<sup>[17]</sup> <sup>19</sup>F, <sup>1</sup>H HOESY NMR analysis of **8**·BF<sub>4</sub> indicated that the BF<sub>4</sub><sup>−</sup> counterion was positioned near the 4-methylstyrene ligand, which is in contrast to the corresponding IPr complex **2**. Brooner, Brown, and Widenhoefer further investigated the solution chemistry of **8**·BF<sub>4</sub>, the SbF<sub>6</sub><sup>−</sup> salt **8**·SbF<sub>6</sub>, and the 2-methyl-2-butene complex  $[\text{Ph}_3\text{PAu}(\eta^2\text{-Me(H)C=CMe}_2)][\text{SbF}_6]$  (**9**·SbF<sub>6</sub>; Scheme 4).<sup>[27]</sup> The complexes **8** and **9** were thermally unstable and decomposed above  $-20^\circ\text{C}$  to form the bis(triphenylphosphine) gold cation  $[(\text{Ph}_3\text{P})_2\text{Au}][\text{SbF}_6]$ . The  $\pi$  ligands of these complexes were weakly bound and competitively displaced by weak anionic ligands such as triflate and bis(triflamide). In the case of the complexes **8**, low-temperature ( $\leq -80^\circ\text{C}$ ) <sup>31</sup>P NMR analysis revealed the presence of both the  $\pi$ -alkene complex and a second complex, presumably free or solvated  $[\text{Ph}_3\text{PAu}]^+$ .<sup>[27]</sup>

### 3. $\pi$ -Alkyne Complexes

#### 3.1. Internal Alkynes

##### 3.1.1. NHC Complexes

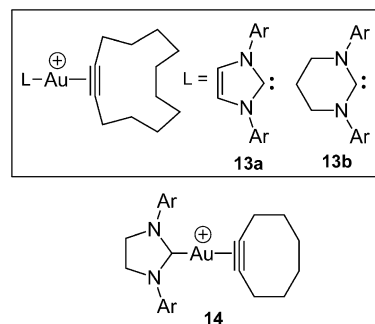
In 2007, Sadighi and co-workers reported isolation of the cationic gold alkyne complex  $[(\text{SIPr})\text{Au}(\eta^2\text{-EtC}\equiv\text{CEt})][\text{BF}_4]$  (**10**) by chloride abstraction from  $[(\text{SIPr})\text{AuCl}]$  with AgBF<sub>4</sub> in the presence of 3-hexyne (Scheme 5).<sup>[14]</sup> The following year,



**Scheme 5.** Cationic gold complexes containing an NHC ligand and an acyclic  $\pi$ -alkyne ligand (Ar = 2,6-diisopropylphenyl).

Bertrand et al. reported the synthesis of the analogous cyclic alkyl amino carbene complex  $[(\text{CAAC})\text{Au}(\eta^2\text{-EtC}\equiv\text{CEt})][\text{B}(\text{C}_6\text{F}_5)_4]$  (**11**) by ligand displacement from the corresponding  $\pi$ -toluene complex with 3-hexyne.<sup>[28]</sup> For **10**, **11**, and the corresponding IPr complex  $[(\text{IPr})\text{Au}(\eta^2\text{-EtC}\equiv\text{CEt})][\text{SbF}_6]$ ,<sup>[29]</sup> the resonances of the alkyne carbon atom were shifted downfield by ca. 6.5 ppm relative to free 3-hexyne ( $\delta = 81.0$  ppm) in the <sup>13</sup>C NMR spectrum. Kinetic analysis of the intermolecular exchange of 2-hexyne with  $[(\text{IPr})\text{Au}(\eta^2\text{-MeC}\equiv\text{CnPr})][\text{BF}_4]$  (**12**) reported by Macchioni and co-workers established the presence of a [2-hexyne]-dependent pathway with an energy barrier of  $\Delta G^\ddagger_{298\text{K}} = 15.5$  kcal mol<sup>−1</sup>,<sup>[30]</sup> similar to that of alkene exchange with IPr gold complexes.<sup>[19]</sup>

In 2009, Fürstner and co-workers reported the synthesis and solid-state structures of the thermally sensitive, cationic gold  $\pi$ -cyclododecyne complexes **13a** and **13b** which contained an NHC ligand (Scheme 6 and Figure 3).<sup>[31]</sup> The C $\equiv$ C bond of the IPr complex **13a** is not significantly different and



**Scheme 6.** Cationic gold complexes containing an NHC ligand and a cyclic  $\pi$ -alkyne ligand (Ar = 2,6-diisopropylphenyl).

the C $\equiv$ C–C angles ( $168^\circ$ ) are diminished slightly relative to free cyclododecyne ( $176^\circ$ ). The greater electron-donor ability of the carbene ligand of **13b** relative to the IPr ligand of **13a** was reflected in the greater shielding of the resonances of the alkyne carbon atoms of **13b** ( $\delta = 86.6$  ppm) relative to **13a** ( $\delta = 88.0$  ppm) in the <sup>13</sup>C NMR spectra, but was less apparent in the solid state. The C–C bond length of **13b** was not significantly different from that of **13a**, and the greater compression of the C $\equiv$ C–C angles of **13b** ( $160^\circ$ ) was attributed



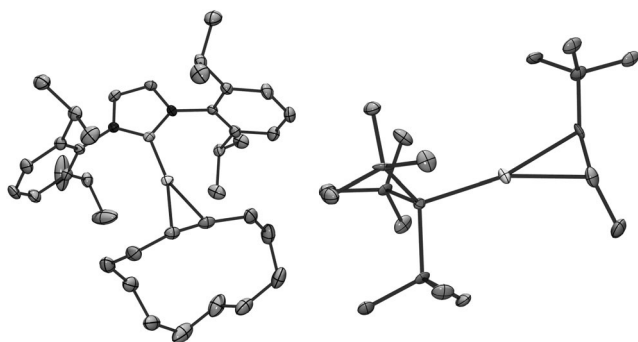
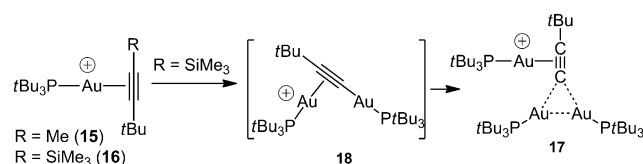


**Figure 3.** ORTEP diagrams of the cationic gold  $\pi$ -alkyne complexes **13a** (left structure) and **15** (right structure). Hydrogen atoms and counterions omitted for clarity. Thermal ellipsoids shown at 50% probability.

to steric rather than electronic effects. Dias and co-workers have recently reported the synthesis and solid-state structure of the analogous cyclooctyne complex  $[(\text{SiPr})\text{Au}(\eta^2\text{-cyclooctyne})][\text{SbF}_6]$  (**14**), which, in contrast to **13a** and **13b**, was thermally stable in solution (Scheme 6).<sup>[32]</sup>

### 3.1.2. Hindered Alkyl Phosphine Complexes

In 2010, Hooper, Green, and Russell reported the synthesis and solid-state characterization of the gold  $\pi$ -alkyne complexes  $[(\text{PtBu}_3)\text{Au}(\text{RC}\equiv\text{CCMe}_3)][\text{SbF}_6]$  [ $\text{R} = \text{Me}$  (**15**),  $\text{SiMe}_3$  (**16**); Scheme 7].<sup>[33]</sup> Brown and Widenhoefer subse-



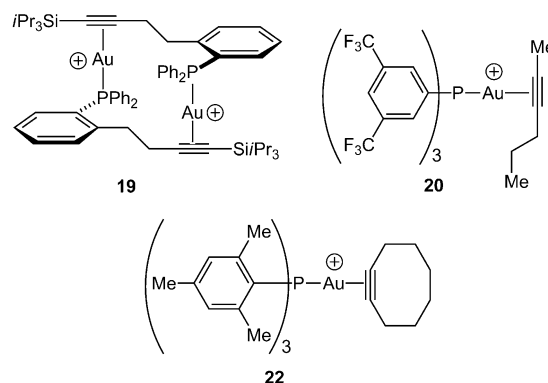
**Scheme 7.** Cationic gold  $\pi$ -alkyne complexes containing an alkylphosphine ligand and the desilylation and aggregation of the gold  $\pi$ -alkyne complex **16**.

quently reported the synthesis and solution structure of gold  $\pi$ -alkyne complexes of the form  $[(\text{P1})\text{Au}(\text{R}^1\text{C}\equiv\text{CR}^2)][\text{SbF}_6]$  [ $\text{R}^1 = \text{Me}$ ,  $\text{R}^2 = \text{Me}$ ,  $n\text{Pr}$ ,  $t\text{Bu}$ ,  $\text{Ph}$ ;  $\text{R}^1 = \text{R}^2 = \text{Et}$ ].<sup>[29]</sup> The resonances of the alkyne sp-carbon atoms of these phosphine complexes were deshielded by ca. 4 ppm ( $\delta = 91.5$  ppm) relative to the corresponding IPr complexes. The X-ray structure of **15** revealed symmetrical coordination of the 4,4-dimethylpent-2-yne ligand to gold with no significant lengthening of the  $\text{C}\equiv\text{C}$  bond relative to free 4,4-dimethylpent-2-yne (Figure 3), although the alkyne substituents were bent away from the  $[(\text{PtBu}_3)\text{Au}]$  moiety ( $\text{C}\equiv\text{C}-\text{C}$ :  $165\text{--}168^\circ$ ). The silyl-acetylene complex **16** was thermally unstable and underwent desilylation to form the trinuclear acetylide complex **17**, presumably via the  $\sigma,\pi$ -acetylide complex **18**. Both **17** and **18** were synthesized independently and structurally characterized (Scheme 7). Macchioni and co-workers analyzed the anion/cation structure of the 3-hexyne complexes  $[(\text{L})\text{Au}(\pi\text{-EtC}\equiv\text{CEt})][\text{BF}_4]$  [ $\text{L} = \text{PtBu}_3$ ,  $\text{P1}$ ] by  $^{19}\text{F}$ ,  $^1\text{H}$  HOESY NMR

spectroscopy and found the counterion positioned primarily near the alkyne ligand.<sup>[34]</sup>

### 3.1.3. Triarylphosphine Complexes

As was the case with gold  $\pi$ -alkene complexes, well-defined examples of cationic gold  $\pi$ -alkyne complexes containing triarylphosphine ligands are scarce. In 2008, Shapiro and Toste reported the isolation and X-ray crystal structure of the dimeric gold  $\pi$ -alkyne complex **19** which contains a triarylphosphine ligand tethered to a (triisopropyl)silyl-acetylene moiety (Scheme 8).<sup>[26]</sup> In the solid state, gold is  $\eta^2$ -



**Scheme 8.** Cationic gold  $\pi$ -alkyne complexes that contain a triarylphosphine ligand.

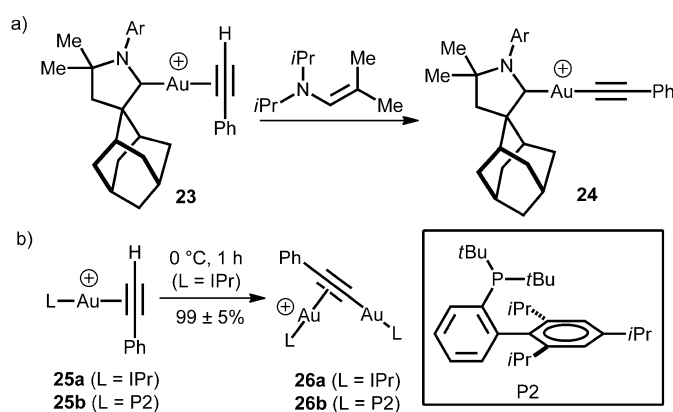
bound to the silylalkyne moiety but is slipped toward the triisopropylsilyl group through a shorter  $\text{Au}-\text{C}(\text{Si})$  and longer  $\text{Au}-\text{C}(\text{C})$  bond ( $\Delta d = 0.073$  Å) with the alkyne substituents bent away from gold [ $\text{C}\equiv\text{C}-\text{C}$ :  $167.2^\circ$ ,  $\text{C}\equiv\text{C}-\text{Si}$ :  $164.4^\circ$ ]. Like the corresponding  $\pi$ -alkene complex **7**, detailed characterization of **19** in solution was precluded by facile disproportionation.

In 2010, Macchioni and co-workers reported in situ generation of the thermally sensitive triarylphosphine gold  $\pi$ -alkyne complex  $[\text{Ar}_3\text{PAu}(\eta^2\text{-MeC}\equiv\text{CnPr})][\text{BF}_4]$  [ $\text{Ar} = 3,5$ -bis(trifluoromethyl)phenyl (**20**)], which was characterized without isolation at  $-69^\circ\text{C}$ .<sup>[30]</sup> Subsequently, Brooner, Brown, and Widenhoefer reported the in situ generation and spectral analysis of the related triphenylphosphine complex  $[\text{Ph}_3\text{PAu}(\eta^2\text{-EtC}\equiv\text{CEt})][\text{SbF}_6]$  (**21**).<sup>[27]</sup> Deshielding of the resonances of the alkyne carbon atoms of **20** and **21** in the  $^{13}\text{C}$  NMR spectra was similar to that of the  $\text{P1}$  and  $\text{PtBu}_3$  complexes. In addition,  $^{19}\text{F}$ ,  $^1\text{H}$  HOESY analysis of **20** indicated that the  $\text{BF}_4^-$  counterion was located near the gold atom in an area between the phosphine and alkyne ligands. Both **20** and **21** were thermally sensitive and decomposed in solution to form the corresponding bis(triarylphosphine) gold cations  $[\text{L}_2\text{Au}]^+$ . Kinetic analysis of intermolecular alkyne exchange with **20** and **21** established associative pathways with energy barriers of  $\Delta G^\ddagger_{204\text{K}} = 9.7$  kcal  $\text{mol}^{-1}$  and  $\Delta G^\ddagger_{188\text{K}} = 9.1$  kcal  $\text{mol}^{-1}$ , respectively. Dias and co-workers have recently reported synthesis and structural characterization of the cyclooctyne complex  $[(\text{Mes}_3\text{P})\text{Au}(\eta^2\text{-cyclooctyne})][\text{SbF}_6]$

(**22**; Scheme 8).<sup>[32]</sup> Although **22** decomposed slowly in solution at room temperature, it is significantly more stable than the 3-hexyne complexes **20** and **21**, presumably because of the more electron-rich trimesitylphosphine ligand. The alkyne carbon atoms of **22** were less shielded ( $\delta = 101.9$  ppm) than were those of the corresponding NHC complex **14** ( $\delta = 97.4$  ppm) in the  $^{13}\text{C}$  NMR spectrum, but were more shielded than were those of the bis(cyclooctyne) complex  $[\text{Au}(\eta^2\text{-cyclooctyne})][\text{SbF}_6]$  cyclooctyne ( $\delta = 110.1$  ppm).<sup>[35]</sup>

### 3.2. Terminal Alkynes

In 2007, Bertrand and co-workers reported the synthesis of the thermally stable gold  $\eta^2$ -phenylacetylene complex **23** containing a cyclic alkyl amino carbene (CAAC) ligand (Scheme 9).<sup>[36]</sup> In the  $^{13}\text{C}$  NMR spectrum of **23**, the resonance



**Scheme 9.** Gold  $\pi$ -terminal-alkyne complexes **23** and **25** and their conversion into gold acetylide complexes (Ar = 2,6-diisopropylphenyl).

of the terminal alkyne carbon atom was shifted upfield ( $\Delta\delta = -6.3$  ppm) and that of the internal alkyne carbon atom was shifted downfield ( $\Delta\delta = 11.3$  ppm) relative to free phenylacetylene. The one-bond alkyne C-H coupling constant ( $^1J_{\text{CH}} = 262$  Hz) of **23** was undiminished relative to free phenylacetylene, thus pointing to  $sp$  hybridization and nominal  $\pi$  backbonding. Treatment of **23** with an exogenous enamine formed the corresponding neutral gold acetylide complex **24** (Scheme 9a).

In 2011, Brown and Widenhoefer reported the in situ generation of thermally sensitive gold  $\pi$ -arylacetylene complexes  $[(\text{IPr})\text{Au}(\eta^2\text{-HC}\equiv\text{C-4-C}_6\text{H}_4\text{-R})][\text{SbF}_6]$  [R = H (**25a**), Me, OMe, Br,  $\text{CF}_3$ ; Scheme 9] which were characterized without isolation at  $-60^\circ\text{C}$ .<sup>[37]</sup> The  $^1J_{\text{C}\equiv\text{C}}$  coupling constant of the phenylacetylene ligand of **25a** (133.8 Hz) was diminished relative to free phenylacetylene (175.9 Hz) and Hammett analysis of the binding affinities of *para*-substituted aryl acetylenes to  $[(\text{IPr})\text{Au}]^+$  revealed a reaction constant of  $\rho = -2.1$ , which was attenuated relative to the corresponding vinyl arene series.<sup>[19]</sup> These observations suggest the more significant contribution of  $\pi$  backbonding to the gold-alkene bond relative to the gold-alkyne bond. Warming a solution of **25a** at  $0^\circ\text{C}$  for 1 hour led to C(sp)-H bond cleavage and

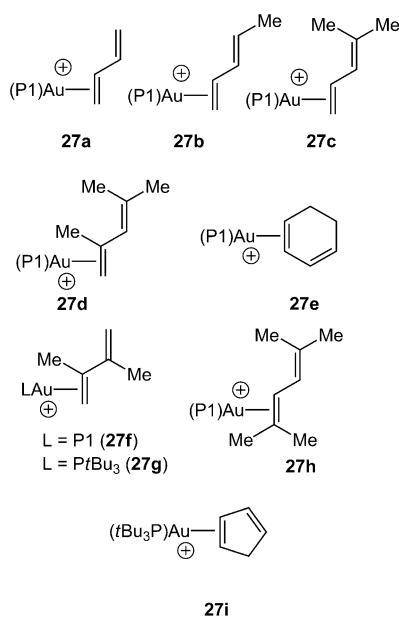
aggregation to form the dinuclear gold(I)  $\sigma,\pi$ -acetylide complex **26a** in 99% yield with concomitant formation of strong Brønsted acid (Scheme 9b).<sup>[37]</sup> Very recently, Obradors and Echavaren have reported generation and low-temperature characterization of the thermally sensitive phenylacetylene complex **25b** and the conversion of **25b** into the  $\sigma,\pi$ -acetylide complex **26b**.<sup>[38,39]</sup>

### 3.3. Alkyne versus Alkene Binding

On the basis of computational analyses<sup>[10–12]</sup> it has been generally assumed that alkenes bind more strongly to cationic gold(I) centers than do alkynes. Supporting this contention, in 2008 Echavarren and co-workers reported that reaction of  $[(\text{P}1)\text{Au}(\text{NCCH}_3)][\text{SbF}_6]$  with a terminally unsubstituted 1,7-enyne led to preferential coordination of the C=C moiety to gold.<sup>[40]</sup> To evaluate the binding affinities of alkynes and alkenes to gold in a more substantive manner, Brown, Dickens, and Widenhoefer determined the relative binding affinities of a number of alkenes and alkynes to both the  $[(\text{P}1)\text{Au}]^+$  and  $[(\text{IPr})\text{Au}]^+$  fragments.<sup>[19,24,29]</sup> Comparison of these data revealed that the superior binding affinity of alkenes relative to alkynes is not a general phenomenon. In fact, the binding affinity of 3-hexyne to both  $[(\text{IPr})\text{Au}]^+$  and  $[(\text{P}1)\text{Au}]^+$  exceeded that of any alkene. Rather, the effect of alkene or alkyne substitution on binding affinity is greater than is the inherent difference between the binding affinities of alkenes and alkynes to gold(I). These conclusions were corroborated by a subsequent analysis of gas-phase alkyne binding energies to the  $[(\text{PMe}_3)_3\text{Au}]^+$  fragment as determined by mass spectrometry.<sup>[41]</sup>

## 4. $\pi$ -1,3-Diene Complexes

In contrast to simple monoene and monoyne complexes of gold, complexation of a 1,3-diene to gold introduces the possibilities of multiple coordination modes and dynamic interconversion between these species. However, prior to 2011, gold  $\pi$ -1,3-diene complexes remained unknown. In this year, Widenhoefer and Brooner reported isolation of the cationic gold  $\pi$ -1,3-diene complexes **27a–f**, including X-ray analyses of **27a–c**,<sup>[42]</sup> while Russell, Green, and co-workers reported isolation and structural characterization of the complexes **27g–i** (Scheme 10).<sup>[43,44]</sup> In all cases, the diene binds to gold in an  $\eta^2$  fashion and in the case of differentially substituted dienes, gold binds to the less substituted C=C bond of the diene. In these latter cases, solution and solid-state analyses point to a bonding model involving donation of electron density from the uncomplexed to the complexed C=C bond. For example, in the  $^{13}\text{C}$  NMR spectrum of the *trans*-1,3-pentadiene complex **27b**, the C1 diene resonance was shifted upfield ( $\Delta\delta = -24$  ppm), the C2 diene resonance was unperturbed ( $\Delta\delta < 1$ ), and the C4 diene resonance was shifted downfield ( $\Delta\delta = 14$  ppm) relative to free diene.<sup>[42]</sup> In the solid state, the 1,3-pentadiene ligand of **27b** was bound unsymmetrically to gold through a shorter Au–C1 and longer Au–C2 interaction ( $\Delta d = 0.113$  Å; Figure 4). The coordinated



**Scheme 10.** Cationic gold  $\eta^2$ -diene complexes.

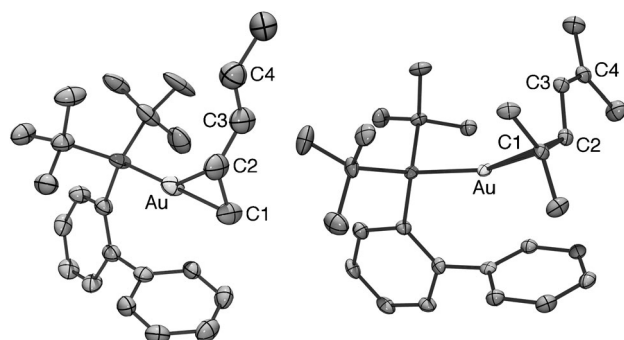
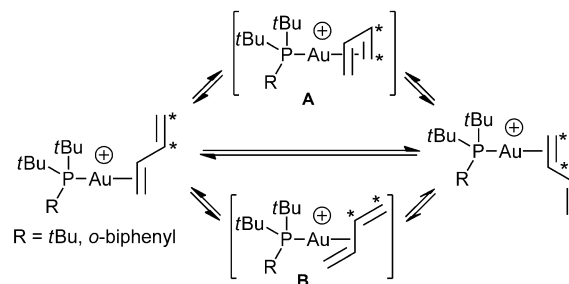


**Figure 4.** ORTEP diagrams of the gold  $\eta^2$ -diene complexes **27b** (left) and **27h** (right). Hydrogen atoms and counterions omitted for clarity. Thermal ellipsoids shown at 50% probability.

C1=C2 bond of the diene is elongated relative to the uncomplexed C3=C4 bond ( $\Delta d = 0.049$  Å), and the C2–C3 bond is unusually short (1.394 Å). In contrast, the terminally tetrasubstituted diene ligand of complex **27h** behaves as an isolated C=C bond without donation from the uncomplexed C=C bond.<sup>[43]</sup> Specifically, the solid-state structure of **27h** revealed that gold was slipped toward the interior of the diene, bonding through a shorter Au–C2 and longer Au–C1 bond ( $\Delta d = 0.65$  Å), and the C3–C4 bond length was typical of a conjugated C–C bond (1.464 Å; Figure 4).

Cationic gold  $\eta^2$ -diene complexes underwent both inter- and intramolecular exchange of the complexed and uncomplexed diene C=C bonds. Kinetic analysis of the intermolecular exchange of 2,4-dimethyl-1,3-pentadiene with **27d** was consistent with an associative pathway via a cationic bis( $\eta^2$ -diene) complex with an energy barrier of  $\Delta G^\ddagger_{298\text{K}} = 14.4$  kcal mol<sup>−1</sup>. In comparison, energy barriers for intramolecular exchange of the complexed and uncomplexed C=C bonds of the diene ligand ranged from  $\Delta G^\ddagger_{214\text{K}} = 9.6$  kcal mol<sup>−1</sup> for the 1,3-butadiene complex **27a** to  $\Delta G^\ddagger_{261\text{K}} =$

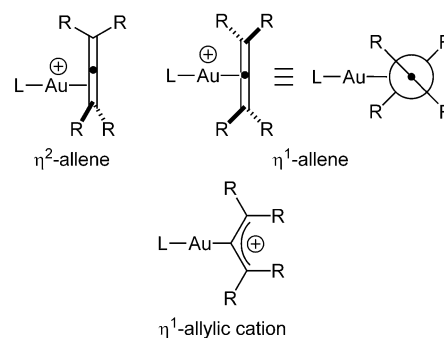
11.9 kcal mol<sup>−1</sup> for 2,3-dimethyl-1,3-butadiene complex **27f**. Brooner and Widenhoefer proposed a mechanism for intramolecular C=C bond exchange involving 16-electron  $\eta^4$ -diene intermediates such as **A**, which are akin to the bis( $\eta^2$ -diene) intermediates involved in intermolecular diene exchange (Scheme 11).<sup>[42]</sup> Conversely, on the basis of DFT calculations, Russell, Green, and co-workers proposed that C=C bond exchange occurred via a transition state such as **B** in which the diene is  $\eta^2$ -bound to the central C2–C3 bond of the diene (Scheme 11).<sup>[43]</sup>



**Scheme 11.** Potential pathways for intramolecular C=C bond exchange in cationic gold  $\eta^2$ -diene complexes. Carbon atoms labeled for clarity only.

## 5. $\pi$ -Allene Complexes

Gold(I)  $\pi$ -allene complexes have attracted particular interest computationally owing both to the widespread utilization of allenes in gold(I)  $\pi$ -activation catalysis<sup>[3]</sup> and to the potential for multiple isomeric coordination modes, all of which have been invoked as reactive intermediates in

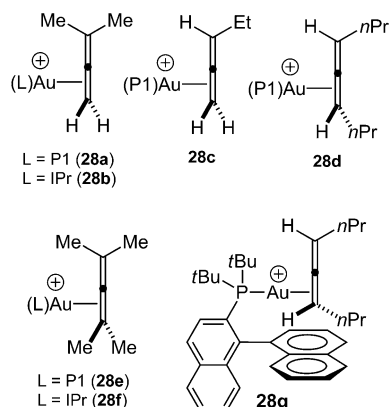


**Scheme 12.** Potential coordination modes accessible to gold  $\pi$ -allene complexes.

gold(I)-catalyzed  $\pi$ -activation processes (Scheme 12).<sup>[45–47]</sup> Most notably, independent DFT calculations of the cationic gold(I)  $\pi$ -2,3-pentadiene complexes  $[(L)Au\{\pi\text{-Me(H)C}=\text{C}=\text{C(H)Me}\}]^+$  ( $L = \text{PMe}_3$ ,<sup>[45]</sup>  $\text{PPh}_3$ )<sup>[46]</sup> identified the *cis,cis*- $\eta^1$ -allylic cation as the lowest energy intermediate, lying less than 6.7 kcal mol<sup>−1</sup> above the  $\eta^2$ -allene ground state and accessed through chiral  $\eta^1$ -allene transition states with activation barriers of 7.9 ( $L = \text{PMe}_3$ ) and 11.6 ( $L = \text{PPh}_3$ ) kcal mol<sup>−1</sup>.

Toward an experimental understanding of the structure and behavior of gold  $\pi$ -allene complexes, Widenhoefer and

co-workers synthesized the cationic gold(I) complexes **28a–g** which contained an aliphatic  $\pi$ -allene ligand and an IPr, P1, or  $P(tBu)_2o$ -binaphthyl ligand (Scheme 13).<sup>[48]</sup> In the solid state, the allene ligand of **28a** binds unsymmetrically to gold through the less-substituted C1=C2  $\pi$  bond with a shorter Au–C1 and a longer Au–C2 interaction ( $\Delta d = 0.116$  Å; Figure 5).



**Scheme 13.** Cationic gold  $\pi$ -allene complexes.

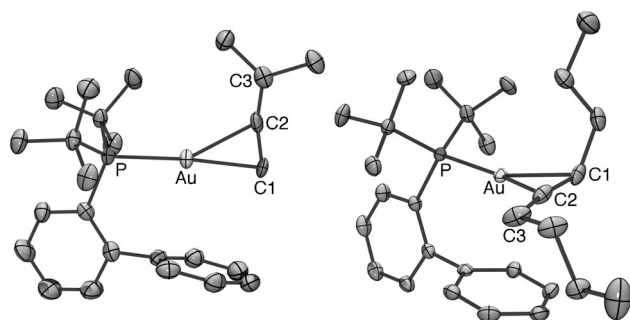
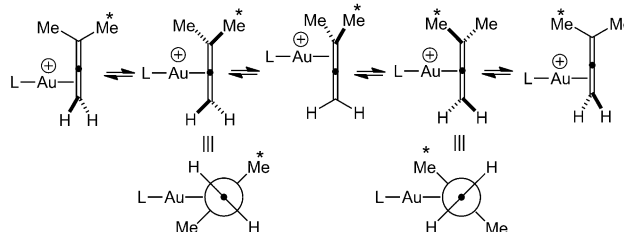


**Figure 5.** ORTEP diagrams of the gold  $\pi$ -allene complexes **28a** (left) and **28d** (right). Hydrogen atoms and counterions omitted for clarity. Thermal ellipsoids shown at 50% probability.

The coordinated C1=C2 bond is elongated by about 0.03 Å relative to the uncomplexed C2=C3 bond, and the allenyl unit is bent with a C1–C2–C3 angle of 165°. In comparison, the 4,5-nonadiene ligand of **28d** binds to gold through a shorter Au–C2 and a longer Au–C1 interaction ( $\Delta d = 0.054$  Å) and **28d** crystallizes exclusively as the diastereomer in which gold is bound to the C1=C2  $\pi$  face *trans* to the C3 *n*-propyl group (Figure 5). In solution, the allene ligand of **28a** binds to gold through the less-substituted C1=C2 bond without detectable concentrations of the C2=C3-bound regioisomer. In comparison, the complex **28d** exists in solution as an equilibrating mixture of *cis* and *trans* diastereomers that differ in energy by less than 0.5 kcal mol<sup>–1</sup>.

Cationic gold  $\pi$ -allene complexes underwent both inter- and intramolecular exchange of the complexed and uncomplexed allene C=C bonds. Kinetic analysis of intermolecular allene exchange established the presence of competing [allene]-independent and [allene]-dependent pathways with energy barriers of  $\Delta G^\ddagger_{298K} = 17.4$ – $18.8$  kcal mol<sup>–1</sup> and 15.2– $17.6$  kcal mol<sup>–1</sup>, respectively. In comparison, intramolecular

exchange of the complexed and uncomplexed allene C=C bonds occurred with energy barriers that ranged from  $\Delta G^\ddagger_{203K} \approx 9$  kcal mol<sup>–1</sup> in the case of **28d** to  $\Delta G^\ddagger_{258K} = 11.5$  kcal mol<sup>–1</sup> in the case of **28b**. Intramolecular C=C bond exchange was proposed to occur through  $\eta^1$ -allene intermediates or transition states which retained a staggered (chiral) arrangement of the allene substituents (Scheme 14). The participation of an  $\eta^1$ -allylic cation species in the low-energy



**Scheme 14.** Proposed mechanism for  $\pi$ -face exchange in cationic gold  $\pi$ -allene complexes involving staggered  $\eta^1$ -allene intermediates or transition states. Carbon atom labeled with a star for clarity only.

$\pi$ -face exchange processes was confidently excluded through analysis of **28g**, which possesses elements of chirality in both the phosphine and allene ligands. Specifically, variable-temperature NMR analysis of **28g** revealed facile  $\pi$ -face exchange with no epimerization of the allene ligand below the threshold for [allene]-independent intermolecular ligand exchange ( $\Delta G^\ddagger_{298K} = 17.4$  kcal mol<sup>–1</sup>). Both the absence of a low-energy  $\eta^1$ -allylic cation species, and the failure of the staggered  $\eta^1$ -allene species to evolve into a more stable  $\eta^1$ -allylic cation intermediate are in direct contradiction to computational prediction.<sup>[45–47]</sup>

## 6. $\pi$ -Arene Complexes

In 2006, Echavarren and co-workers reported isolation of the gold  $\pi$ -arene complexes  $[LAu(\pi\text{-arene})][SbF_6]$  [ $L = P1$ , arene = toluene, *p*-xylene;  $L = PCy_2o$ -biphenyl; arene = toluene (**29a**), *p*-xylene (**29b**)] by crystallization of  $[LAuNCCH_3][SbF_6]$  from the appropriate aromatic solvent.<sup>[13]</sup> Solid-state analysis showed Au–Ar<sub>plane</sub> distances of 2.20–2.24 Å with the complexed arene perpendicular to the Au–P bond vector (Figure 6). Bonding of the arene to gold varied from nominal

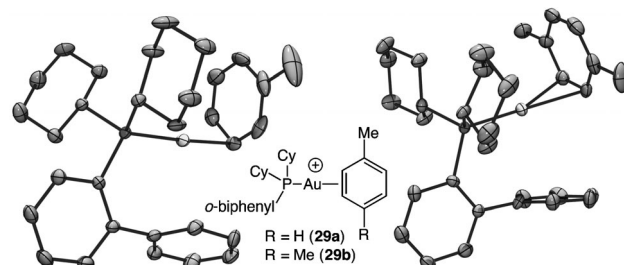


**Figure 6.** Skeletal representation and ORTEP diagrams of the complexes **29a** (right) and **29b** (left). Hydrogen atoms and counterions have been omitted for clarity. Thermal ellipsoids shown at 50% probability.



$\eta^1$ -coordination in the case of the toluene complex **29a** in which the primary Au–C interaction is more than 0.27 Å shorter than are the flanking Au–C bonds, to  $\eta^2$ -coordination in the case of the *p*-xylene complex **29b** in which the Au–C bond lengths are not significantly different. The room temperature NMR spectra of these complexes displayed broad resonances, presumably because of the fluxionality of the arene ligands.<sup>[13]</sup> Bertrand and co-workers subsequently reported isolation and X-ray analysis of the related NHC complex  $[(\text{CAAC})\text{Au}(\eta^2\text{-toluene})][\text{B}(\text{C}_6\text{F}_5)_4]$  (**30**). Complex **30** was stable indefinitely in solution but the arene ligand was rapidly and quantitatively displaced by alkynes.<sup>[36]</sup>

## 7. Complexes with Heteroatom-Substituted $\pi$ Ligands

### 7.1. Enamine Complexes

In 2008, Fürstner et al. reported the synthesis and X-ray crystal structures of cationic triphenylphosphine gold enamine complexes which contained an  $\eta^1$ -2-methyleneimidazoline (**31**) or  $\eta^1$ -tetraaminoallene (**32**) ligand (Figure 7).<sup>[49]</sup> In

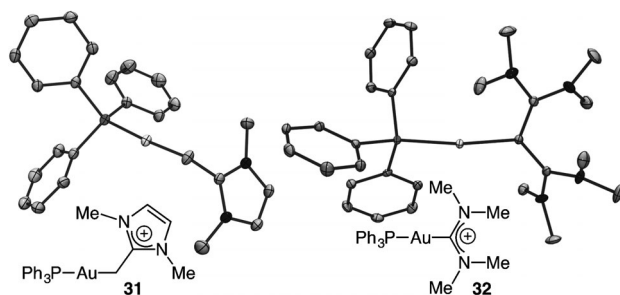


**Figure 7.** Skeletal drawings and ORTEP diagrams of the gold enamine complex **31** and **32**. Hydrogen atoms and counterions have been omitted for clarity. Thermal ellipsoids shown at 50% probability.

contrast to gold complexes of alkyl and aliphatic alkenes, X-ray analysis of these complexes revealed  $\eta^1$  coordination of the nitrogen-substituted alkene with no significant contribution of the corresponding  $\eta^2$  canonical form (Figure 7). The  $\eta^1$ -2-methyleneimidazoline ligand of **31** behaves as an  $\alpha$ -metallated carbon ylide whereas the tetraaminoallene ligand of **32** is best described as a carbodicarbene ligand comprised of a zerovalent central carbon atom with two filled, orthogonal orbitals bound to two diaminocarbene groups. The high thermal stability of these gold enamine complexes in comparison to the aliphatic and aromatic alkene complexes **8** and **9** can be traced the predominant  $\sigma$ -bonding character of enamine complexes, and which are stabilized by decreasing electron density of the  $[(\text{L})\text{Au}]^+$  fragment.<sup>[5]</sup>

### 7.2. Enol Ether Complexes

In the course of their study of gold  $\pi$ -1,3-diene complexes, Russell, Green, and co-workers reported the synthesis and

structure of the 2,3-dimethoxy-1,3-butadiene complex **33**.<sup>[43]</sup> Structural and spectroscopic analysis of **33** revealed significant slippage of the 2,3-dimethoxy-1,3-butadiene ligand toward the  $\text{CH}_2$  terminus with significant contribution of the  $\alpha$ -metallated oxocarbenium ion canonical form (Figure 8). Specifically, the Au–C1 bond of **33** is significantly

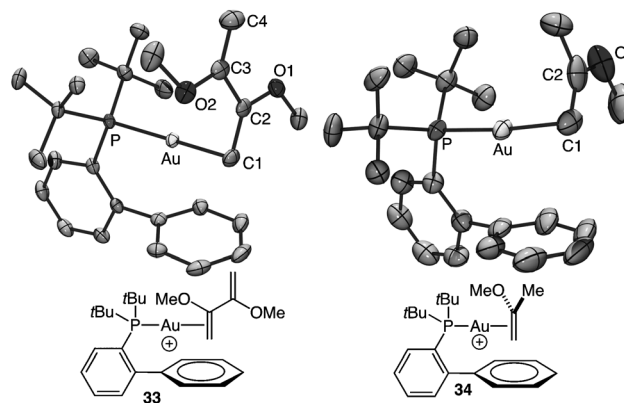


**Figure 8.** Skeletal drawings and ORTEP diagrams of **33** and **34**. Hydrogen atoms and counterion have been omitted for clarity. Thermal ellipsoids shown at 50% probability.

shorter than is the Au–C2 bond ( $\Delta d = 0.368$  Å), the coordinated C1=C2 bond is elongated relative to the uncomplexed C3=C4 bond ( $\Delta d = 0.059$  Å), and the C2=O1 bond is compressed relative to the C3=O2 bond ( $\Delta d = 0.034$  Å). In contrast to gold complexes containing aliphatic 1,3-dienes, room temperature analysis of **33** revealed no evidence for exchange of the complexed and uncomplexed C=C bonds on the NMR timescale.

Jones and co-workers subsequently reported a more extensive study of gold enol ether complexes of the form  $[(\text{L})\text{Au}(\pi\text{-enol ether})][\text{SbF}_6]$  ( $\text{L} = \text{PtBu}_3$ ,  $\text{P1}$ ; enol ether = methoxy- and ethoxypropene, 5-H- and 5-methyl-2,3-dihydrofuran).<sup>[50]</sup> As was the case with **33**, structural and spectroscopic analysis of these complexes revealed significant contribution of the  $\alpha$ -metallated oxocarbenium ion canonical form. For example, X-ray analysis of  $[(\text{P1})\text{Au}(\pi\text{-H}_2\text{C}=\text{C}(\text{OMe})\text{Me})][\text{SbF}_6]$  (**34**) revealed highly unsymmetrical binding of the methoxypropene ligand to gold through a short Au–C1 and long Au–C2 interaction ( $\Delta d = 0.408$  Å) with an elongated C1=C2 bond ( $\Delta d = 0.075$  Å) and a compressed C2=O bond ( $\Delta d = 0.087$  Å) relative to free methoxypropene (Figure 8). This study also provided some interesting comparisons between the behavior of enol ethers and aliphatic alkenes with respect to gold(I). For example, the equilibrium binding affinity of 2-methoxyprop-1-ene to the  $[(\text{P1})\text{Au}]^+$  fragment is approximately 280 times greater than is that of isobutylene, and presumably reflects the greater donicity of the enol ether. Similarly, the energy barrier ( $\Delta G^\ddagger_{297\text{K}} = 15.9$  kcal mol<sup>−1</sup>) and activation parameters ( $\Delta H^\ddagger = 6.7$  kcal mol<sup>−1</sup>;  $\Delta S^\ddagger = -30$  eu) for associative, intermolecular methoxypropene exchange with **34** were similar to those for isobutylene exchange with **5b**.<sup>[24]</sup>

## 8. Summary and Outlook

Building upon the 2006 report from Echavarren and co-workers on the isolation and structural characterization of cationic, two-coordinate gold(I)  $\pi$ -arene complexes, the number of well-defined examples of cationic, two-coordinate gold  $\pi$  complexes has increased dramatically and now include complexes of alkenes, alkynes, conjugated dienes, allenes, enamines, and enol ethers. These activities have been motivated by the proliferation of gold(I)-catalyzed organic transformations, particularly those involving  $\pi$  activation of C–C multiple bonds, and by the central role that two-coordinate gold  $\pi$  complexes are presumed to play in these transformations. One of the key conclusions drawn from these studies is that the 12-electron  $[(L)Au]^+$  fragment is highly electropositive, particularly in the cases where L = phosphine, but in all cases much more so than are the 16-electron  $[L_2M]^+$  (M = Pd, Pt) fragments which have long stood as the benchmarks of electrophilic late-transition-metal species.

The high electrophilicity of gold is evidenced in several ways. The binding affinities of  $\pi$  ligands to  $[(L)Au]^+$  are highly sensitive to the electron density of the  $\pi$  ligand, which points to dominant  $\sigma$  donation of the  $\pi$  ligand in the Chatt-Dewar-Duncanson bonding model. A notable ramification of this bonding behavior is that no cationic, two-coordinate gold ethylene or acetylene complexes have been documented.<sup>[51]</sup> Similarly, polarizable  $\pi$  ligands such as 1,1-disubstituted alkenes, terminally unsubstituted 1,3-dienes, and enol ethers bind unsymmetrically to gold through long and short Au–C bonds which leads to accumulation of positive charge at the distal terminus of the  $\pi$  ligand. Not surprisingly, the stability and reactivity of gold  $\pi$  complexes is also sensitive to the nature of the supporting ligand. Gold  $\pi$  complexes that contain electron-rich, sterically hindered supporting ligands such as IPr and *Pr*Bu<sub>2</sub>O-biphenyl (P1) are typically stable at room temperature in the solid state and in solution, whereas triphenylphosphine gold complexes containing aromatic and aliphatic  $\pi$  ligands decompose in solution above –20 °C and have, to date, escaped isolation. Similarly, gold  $\pi$  complexes containing electron-rich, sterically hindered supporting ligands such as IPr and *Pr*Bu<sub>2</sub>O-biphenyl (P1) undergo intermolecular  $\pi$ -ligand exchange with energy barriers which are approximately 6 kcal mol<sup>–1</sup> greater than those for the corresponding triarylphosphine gold  $\pi$  complexes, although it is not clear whether the origin of this effect is primarily steric or electronic.

Cationic gold  $\eta^2$ -(1,3-dienes) and  $\eta^2$ -allene complexes undergo facile ( $\Delta G^\ddagger = 9$ –12 kcal mol<sup>–1</sup>) exchange of the complexed and uncomplexed C=C bonds. For the  $\pi$ -face exchange of  $\eta^2$ -(1,3-dienes) complexes, mechanisms involving either 16-electron  $\eta^4$  intermediates/transition states or 14-electron  $\eta^2$  intermediates/transition states have been invoked. In comparison,  $\pi$ -face exchange of gold  $\eta^2$ -allene complexes occurs via  $\eta^1$ -allene intermediates/transition states which retain a staggered arrangement of the allene substituents without involvement of achiral  $\eta^1$ -allylic cation intermediates. With the exception of these inter- and intramolecular ligand exchange processes, little is known regarding the reactivity of cationic two-coordinate gold  $\pi$  complexes, most notably the

reactivity of the  $\pi$  ligand toward nucleophilic addition. Although stereochemical analysis of the gold-catalyzed and gold-mediated addition of nucleophiles to C–C multiple bonds support outer-sphere pathways,<sup>[4,5]</sup> the conversion of a cationic gold  $\pi$  complex and nucleophile into the corresponding neutral gold  $\sigma$  complex has not been directly observed, even though the latter complexes are now quite common.<sup>[6]</sup> The primary challenge in this endeavor is that most competent nucleophiles are also good ligands for gold(I) and facile ligand exchange obscures any nucleophilic addition pathways.

*We thank the NSF (CHE-0911265 and CHE-1213957) for supporting our efforts in the area of cationic gold  $\pi$  complexes. R.E.M.B. was supported in part through Charles Bradsher and Joe Taylor Adams Fellowships (Duke University).*

Received: April 24, 2013

Published online: September 18, 2013

- [1] a) D. J. Gorin, B. D. Sherry, F. D. Toste, *Chem. Rev.* **2008**, *108*, 3351–3378; b) A. Arcadi, *Chem. Rev.* **2008**, *108*, 3266–3325; c) Z. Li, C. Brouwer, C. He, *Chem. Rev.* **2008**, *108*, 3239–3265.
- [2] a) P. Y. Toullec, V. Michelet, *Top. Curr. Chem.* **2011**, *302*, 31–80; b) A. Fürstner, P. W. Davies, *Angew. Chem.* **2007**, *119*, 3478–3519; *Angew. Chem. Int. Ed.* **2007**, *46*, 3410–3449; c) E. Jiménez-Núñez, A. M. Echavarren, *Chem. Rev.* **2008**, *108*, 3326–3350.
- [3] a) A. Corma, A. Leyva-Pérez, M. J. Sabater, *Chem. Rev.* **2011**, *111*, 1657–1712; b) N. Krause, C. Winter, *Chem. Rev.* **2011**, *111*, 1994–2009.
- [4] a) Z. Zhang, R. A. Widenhoefer, *Org. Lett.* **2008**, *10*, 2079–2081; b) Z. Zhang, R. A. Widenhoefer, *Angew. Chem.* **2007**, *119*, 287–289; *Angew. Chem. Int. Ed.* **2007**, *46*, 283–285; c) Z. Zhang, C. F. Bender, R. A. Widenhoefer, *J. Am. Chem. Soc.* **2007**, *129*, 14148–14149; d) Z. Zhang, C. Liu, R. E. Kinder, X. Han, H. Qian, R. A. Widenhoefer, *J. Am. Chem. Soc.* **2006**, *128*, 9066–9073; e) Y. Liu, F. Song, Z. Song, M. Liu, B. Yan, *Org. Lett.* **2005**, *7*, 5409–5412; f) J. J. Kennedy-Smith, S. T. Staben, F. D. Toste, *J. Am. Chem. Soc.* **2004**, *126*, 4526–4527; g) A. S. K. Hashmi, J. P. Weyrauch, W. Frey, J. W. Bats, *Org. Lett.* **2004**, *6*, 4391–4394.
- [5] R. L. LaLonde, W. E. Brenzovich, Jr., D. Benitez, E. Tkatchouk, K. Kelley, W. A. Goddard, III, F. D. Toste, *Chem. Sci.* **2010**, *1*, 226–233.
- [6] A. S. K. Hashmi, *Angew. Chem.* **2010**, *122*, 5360–5369; *Angew. Chem. Int. Ed.* **2010**, *49*, 5232–5241.
- [7] a) A. J. Chalk, *J. Am. Chem. Soc.* **1964**, *86*, 4733–4734; b) R. Hüttel, H. Dietl, *Angew. Chem.* **1965**, *77*, 456–456; *Angew. Chem. Int. Ed. Engl.* **1965**, *4*, 438–438.
- [8] R. M. Davila, R. J. Staples, J. P. Fackler, *Organometallics* **1994**, *13*, 418–420.
- [9] For a review and historical perspective of gold  $\pi$  complexes including examples of poorly characterized, cationic bis-(alkene)gold complexes and more detailed discussions of neutral two-coordinate and three-coordinate gold  $\pi$  complexes, see: a) H. Schmidbaur, A. Schier, *Organometallics* **2010**, *29*, 2–23; b) M. A. Cinellu in *Modern Gold Catalyzed Synthesis* (Eds.: A. S. K. Hashmi, D. F. Toste), Wiley-VCH, **2012**, pp. 153–199.
- [10] a) T. Ziegler, A. Rauk, *Inorg. Chem.* **1979**, *18*, 1558–1565; b) R. H. Hertwig, W. Koch, D. Schröder, H. Schwarz, J. Hruák, P. Schwerdtfeger, *J. Phys. Chem.* **1996**, *100*, 12253–12260; c) M. S. Nechaev, V. M. Rayón, G. Frenking, *J. Phys. Chem. A* **2004**, *108*, 3134–3142.

- [11] E. Soriano, J. Marco-Contelles, *Top. Curr. Chem.* **2011**, 302, 1–29, and references therein.
- [12] N. Salvi, L. Belpassi, F. Tarantelli, *Chem. Eur. J.* **2010**, 16, 7231–7240.
- [13] E. Herrero-Gómez, C. Nieto-Oberhuber, S. López, J. Benet-Buchholz, A. M. Echavarren, *Angew. Chem.* **2006**, 118, 5581–5585; *Angew. Chem. Int. Ed.* **2006**, 45, 5455–5459.
- [14] J. A. Akana, K. X. Bhattacharyya, P. Miller, J. P. Sadighi, *J. Am. Chem. Soc.* **2007**, 129, 7736–7737.
- [15] For lead references, see: a) D. Weber, M. A. Tarselli, M. R. Gagné, *Angew. Chem.* **2009**, 121, 5843–5846; *Angew. Chem. Int. Ed.* **2009**, 48, 5733–5736; b) D. Weber, M. R. Gagné, *Org. Lett.* **2009**, 11, 4962–4965; c) G. Seidel, C. W. Lehmann, A. Fürstner, *Angew. Chem.* **2010**, 122, 8644–8648; *Angew. Chem. Int. Ed.* **2010**, 49, 8466–8470; d) A. Himmelsbach, M. Finze, S. Raub, *Angew. Chem.* **2011**, 123, 2676–2679; *Angew. Chem. Int. Ed.* **2011**, 50, 2628–2631; e) A. S. K. Hashmi, I. Braun, M. Rudolph, F. Rominger, *Organometallics* **2012**, 31, 644–661; f) Y. Chen, M. Chen, Y. Liu, *Angew. Chem.* **2012**, 124, 6285–6290; *Angew. Chem. Int. Ed.* **2012**, 51, 6181–6186; g) A. Gómez-Suárez, S. P. Nolan, *Angew. Chem.* **2012**, 124, 8278–8281; *Angew. Chem. Int. Ed.* **2012**, 51, 8156–8159; h) T. J. Brown, D. Weber, M. R. Gagné, R. A. Widenhoefer, *J. Am. Chem. Soc.* **2012**, 134, 9134–9137; i) A. S. K. Hashmi, M. Wietek, I. Braun, P. Nösel, L. Jongbloed, M. Rudolph, F. Rominger, *Adv. Synth. Catal.* **2012**, 354, 555–562; j) A. S. K. Hashmi, I. Braun, P. Nösel, J. Schädlich, M. Wietek, M. Rudolph, F. Rominger, *Angew. Chem.* **2012**, 124, 4532–4536; *Angew. Chem. Int. Ed.* **2012**, 51, 4456–4460; k) D. Weber, T. D. Jones, L. L. Adduci, M. R. Gagné, *Angew. Chem.* **2012**, 124, 2502–2506; *Angew. Chem. Int. Ed.* **2012**, 51, 2452–2456; l) J. E. Heckler, M. Zeller, A. D. Hunter, T. G. Gray, *Angew. Chem.* **2012**, 124, 6026–6030; *Angew. Chem. Int. Ed.* **2012**, 51, 5924–5928; m) D. Weber, M. R. Gagné, *Chem. Sci.* **2013**, 4, 335–338; n) A. Gómez-Suárez, S. Dupuy, A. M. Z. Slawin, S. P. Nolan, *Angew. Chem.* **2013**, 125, 972–976; *Angew. Chem. Int. Ed.* **2013**, 52, 938–942; o) A. Zhdanko, M. E. Maier, *Chem. Eur. J.* **2013**, 19, 3932–3942.
- [16] P. de Frémont, N. Marion, S. P. Nolan, *J. Organomet. Chem.* **2009**, 694, 551–560.
- [17] D. Zuccaccia, L. Belpassi, F. Tarantelli, A. Macchioni, *J. Am. Chem. Soc.* **2009**, 131, 3170–3171.
- [18] N. Salvi, L. Belpassi, D. Zuccaccia, F. Tarantelli, A. Macchioni, *J. Organomet. Chem.* **2010**, 695, 2679–2686.
- [19] T. J. Brown, M. G. Dickens, R. A. Widenhoefer, *J. Am. Chem. Soc.* **2009**, 131, 6350–6351.
- [20] T. Fueno, T. Okuyama, T. Deguchi, J. Furukawa, *J. Am. Chem. Soc.* **1965**, 87, 170–174.
- [21] H. Kurosawa, N. Asada, *J. Organomet. Chem.* **1981**, 217, 259–266.
- [22] H. Kurosawa, T. Majima, N. Asada, *J. Am. Chem. Soc.* **1980**, 102, 6996–7003.
- [23] T. N. Hooper, M. Green, J. E. McGrady, J. R. Patel, C. A. Russell, *Chem. Commun.* **2009**, 3877–3879.
- [24] T. J. Brown, M. G. Dickens, R. A. Widenhoefer, *Chem. Commun.* **2009**, 6451–6453.
- [25] R. E. M. Brooner, R. A. Widenhoefer, *Organometallics* **2012**, 31, 768–771.
- [26] N. D. Shapiro, F. D. Toste, *Proc. Natl. Acad. Sci. USA* **2008**, 105, 2779–2782.
- [27] R. E. M. Brooner, T. J. Brown, R. A. Widenhoefer, *Chem. Eur. J.* **2013**, 19, 8276–8284.
- [28] V. Lavallo, G. D. Frey, B. Donnadiou, M. Soleilhavoup, G. Bertrand, *Angew. Chem.* **2008**, 120, 5302–5306; *Angew. Chem. Int. Ed.* **2008**, 47, 5224–5228.
- [29] T. J. Brown, R. A. Widenhoefer, *J. Organomet. Chem.* **2011**, 696, 1216–1220.
- [30] D. Zuccaccia, L. Belpassi, L. Rocchigiani, F. Tarantelli, A. Macchioni, *Inorg. Chem.* **2010**, 49, 3080–3082.
- [31] S. Flügge, A. Anoop, R. Goddard, W. Thiel, A. Fürstner, *Chem. Eur. J.* **2009**, 15, 8558–8565.
- [32] M. A. Celik, C. Dash, V. A. K. Adiraju, A. Das, M. Yousufuddin, G. Frenking, H. V. R. Dias, *Inorg. Chem.* **2013**, 52, 729–742.
- [33] T. N. Hooper, M. Green, C. A. Russell, *Chem. Commun.* **2010**, 46, 2313–2315.
- [34] G. Ciancaleoni, L. Belpassi, F. Tarantelli, D. Zuccaccia, A. Macchioni, *Dalton Trans.* **2013**, 42, 4122–4131.
- [35] A. Das, C. Dash, M. A. Celik, M. Yousufuddin, G. Frenking, H. V. R. Dias, *Organometallics* **2013**, 32, 3134–3144.
- [36] V. Lavallo, G. D. Frey, S. Kousar, B. Donnadiou, G. Bertrand, *Proc. Natl. Acad. Sci. USA* **2007**, 104, 13569–13573.
- [37] T. J. Brown, R. A. Widenhoefer, *Organometallics* **2011**, 30, 6003–6009.
- [38] C. Obradors, A. M. Echavarren, *Chem. Eur. J.* **2013**, 19, 3547–3551.
- [39] For additional studies of the conversion of terminal alkynes into gold  $\sigma,\pi$ -acetylide complexes in the absence of base, see: a) A. Grirrane, H. Garcia, A. Corma, E. Alvarez, *ACS Catal.* **2011**, 1, 1647–1653; b) A. Simonneau, F. Jaroschik, D. Lesage, M. Karanik, R. Guillot, M. Malacria, J.-C. Tabet, J.-P. Goddard, L. Fensterbank, V. Gandon, Y. Gimbert, *Chem. Sci.* **2011**, 2, 2417–2422.
- [40] M. García-Mota, N. Cabello, F. Maseras, A. M. Echavarren, J. Pérez-Ramírez, N. López, *ChemPhysChem* **2008**, 9, 1624–1629.
- [41] L. Jasíková, J. Roithová, *Organometallics* **2012**, 31, 1935–1942.
- [42] R. E. M. Brooner, R. A. Widenhoefer, *Organometallics* **2011**, 30, 3182–3193.
- [43] R. A. Sanguramath, T. N. Hooper, C. P. Butts, M. Green, J. E. McGrady, C. A. Russell, *Angew. Chem.* **2011**, 123, 7734–7737; *Angew. Chem. Int. Ed.* **2011**, 50, 7592–7595.
- [44] R. A. Sanguramath, S. K. Patra, M. Green, C. A. Russell, *Chem. Commun.* **2012**, 48, 1060–1062.
- [45] V. Gandon, G. Lemièrre, A. Hours, L. Fensterbank, M. Malacria, *Angew. Chem.* **2008**, 120, 7644–7648; *Angew. Chem. Int. Ed.* **2008**, 47, 7534–7538.
- [46] Z. J. Wang, D. Benitez, E. Tkatchouk, W. A. Goddard, F. D. Toste, *J. Am. Chem. Soc.* **2010**, 132, 13064–13071.
- [47] For recent reviews, see: a) M. Malacria, L. Fensterbank, V. Gandon, *Top. Curr. Chem.* **2011**, 302, 157–182; b) S. Montserrat, G. Ujaque, F. López, J. L. Mascareñas, A. Lledós, *Top. Curr. Chem.* **2011**, 302, 225–248; c) B. Alcaide, P. Almendros, T. M. del Campo, E. Soriano, J. Marco-Contelles, *Top. Curr. Chem.* **2011**, 302, 183–224.
- [48] a) T. J. Brown, A. Sugie, M. G. Dickens, R. A. Widenhoefer, *Organometallics* **2010**, 29, 4207–4209; b) T. J. Brown, A. Sugie, M. G. Dickens, R. A. Widenhoefer, *Chem. Eur. J.* **2012**, 18, 6959–6971.
- [49] A. Fürstner, M. Alcarazo, R. Goddard, C. W. Lehmann, *Angew. Chem.* **2008**, 120, 3254–3258; *Angew. Chem. Int. Ed.* **2008**, 47, 3210–3214.
- [50] a) Y. Zhu, C. S. Day, A. C. Jones, *Organometallics* **2012**, 31, 7332–7335; b) Y. Zhu, C. S. Day, A. C. Jones, *Organometallics* **2013**, 32, 5005–5005.
- [51] Three-coordinate gold ethylene complexes are known: H. V. R. Dias, J. Wu, *Eur. J. Inorg. Chem.* **2008**, 509–522.